1				
2				
3				
4				
5				
6	Comparative St	udy of the Effects of Biocides and Metal Oxide		
7	Nanoparticles on Microbial Community Structure in a Stream			
8	Im	pacted by Hydraulic Fracturing.		
9				
10 11	Rehab K Alhajjar <sup>1</sup> , Ryan B. Ghannam <sup>1</sup> , Jeremy R. Chen See <sup>2</sup> , Olivia G. Wright <sup>2</sup> , Maria Fernanda Campa <sup>3</sup> , Terry C. Hazen <sup>3</sup> , Regina Lamendella <sup>2</sup> , Stephen M. Techtmann <sup>1</sup> *			
12				
13	<sup>1</sup> Department of Biological Sciences, Michigan Technological University, Houghton MI			
14	<sup>2</sup> Department of Biology, Juniata College, Huntingdon, PA			
15 16	<sup>3</sup> Department of Civil and E Knoxville, TN	Environmental Engineering, University of Tennessee, Knoxville,		
17	Running Title: Biocide and Nanoparticle Impacts on Stream Microbes			
18	Keywords: Biocides, Nanoparticles, antimicrobials, 16S rRNA			
19				
20 21 22 23 24 25 26	*Corresponding Author:	Stephen M. Techtmann 740 Dow ESE building 1400 Townsend Drive Houghton, MI, 49931 (906) 487-3250 smtechtm@mtu.edu		
27	There are no competing interests			

### **Abstract**

28

Our study goal was to investigate the impact of biocides and nanoparticles (NPs) on the 29 microbial diversity in a hydraulic fracturing impacted stream. Biocides and NPs are known for 30 their antimicrobial properties and controlling microbial growth. Previous work has shown that 31 32 biocides can alter the microbial community composition of stream water and may select for biocide-resistant bacteria. Additional studies have shown that nanoparticles can also alter 33 microbial community composition. However, previous work has often focused on the response to 34 a single compound. Here we provide a more thorough analysis of the microbial community 35 response to three different biocides and three different nanoparticles. A microcosm-based study 36 was undertaken that exposed stream microbial communities to either biocides or NPs. Our results 37 showed a decrease in bacterial abundance with different types of nanoparticles, but an increase in 38 microbial abundance in biocide-amended treatments. The microbial community composition 39 (MCC) was distinct from the controls in all biocide and NP treatments, which resulted in 40 41 differentially enriched taxa in the treatments compared to the controls. Our results indicate that NPs slightly altered the MCC compared to the biocide-treated microcosms. After 14 days, the 42 MCC in the nanoparticle-treated conditions was similar to the MCC in the control. Conversely, 43 the MCC in the biocide-treated microcosms was distinct from the controls at day 14 and distinct 44 45 from all conditions at day 0. This finding may point to the use of NPs as an alternative to biocides in some settings. 46 47

#### Introduction

48

49

50

51

52

53

54

55

56

57

58

59

60

61

62

63

64

65

66

67

68

69

70

Biocides and nanoparticles are known for their antimicrobial properties and are used in controlling microbial growth (Maillard, 2005, Fernando et al., 2018a, Fernando et al., 2018b). If released to the environment, biocides and nanoparticles have the potential for transient and longterm effects on the health of the environment. Biocides are chemical substances used in industrial and household applications to control a wide range of microorganisms (Fink, 2013). The common use of biocides in diverse industries is due in part to their effectiveness and low cost (Guardiola et al., 2012, Levy, 2002). There are more than 23 types of biocides used in different applications (Guardiola et al., 2012). Quaternary ammonium compounds (QACs), glutaraldehyde (GA), Triclosan (TCS), Triclocarban (TCC), chlorine dioxide, and other biocides are commonly used in both household and industrial applications (Levy, 2002). The widespread use of biocides and their release to the environment have led to ecological problems (Kahrilas et al., 2015). Of particular interest to our study is the use of biocides in the oil and gas industry, specifically, in hydraulic fracturing (HF), the process in which highly pressurized water, sand, and a mixture of chemicals are injected into oil and gas harboring shales to release the oil and gas. Biocides are commonly used in hydraulic fracturing to control microbial growth and prevent biofouling. Hydraulic fracturing activity has been shown to alter the response of stream microorganisms to biocides (Mumford et al., 2018, Campa et al., 2018, Campa et al., 2019). The biocide 2, 2dibromo-3-nitrilopropionamide (DBNPA) is used in the paper and oil and gas industries for disinfection of industrial water systems and equipment (Chattopadhyay et al., 2004, Siddiqui et al., 2017). Glutaraldehyde (GA) and DBNPA are two of the most commonly used biocides in hydraulic fracturing operations (Kahrilas et al., 2015). The release of biocides such as GA and

DBNPA into aquatic environments can cause shifts in the microbial community composition through inactivation of certain microbes. For example, Mumford et al (2018) demonstrated the potential for biocides to decrease iron reduction rates (Mumford et al., 2018). Another study has shown that GA amendment resulted in changes to microbial community structure in stream microbial communities (Campa et al., 2018). In a microcosm-based study, differences were observed in the microbial community response to GA depending on the level of hydraulic fracturing activity in the watershed along with past contamination (spills), with streams previously exposed to hydraulic fracturing wastewater being more resistant to GA addition (Campa et al., 2018). Furthermore, it has been proposed that biocide use associated with hydraulic fracturing operations could lead to antimicrobial resistance in adjacent streams (Campa et al., 2019c). Nanoparticles (NPs) are substances with nanoscale diameters. The design and shape of NPs play an important role in the activity and function of these particles (Liu et al., 2012, Kanchi and Khan, 2020). Engineered nanoparticle materials, such as silver, titanium dioxide (TiO<sub>2</sub>), and zinc dioxide (ZnO), have antimicrobial properties (Paterson et al., 2011, Li et al., 2008). Metal oxides NPs and other metals, such as silver and copper, are commonly used to control microbial activity (Wang et al., 2017). For example, one study showed that organic–inorganic hybrid nanomaterials can be used for many applications in the medical field and in the treatment of wastewater due to their antimicrobial properties and their great ion exchange capacity (Ahamed et al., 2016). Metal and metal oxides of NPs have been reported to be toxic to microbes through diverse mechanisms (Slavin et al., 2017). These mechanisms include production of reactive oxygen species (TiO<sub>2</sub>, ZnO), compromising of the cell envelope (ZnO and Ag), among other mechanisms (Slavin et al., 2017). Similarly, silica nanoparticles have antimicrobial activity and are considered safe with

71

72

73

74

75

76

77

78

79

80

81

82

83

84

85

86

87

88

89

90

91

92

nonporous silica nanoparticles being considered a promising drug carrier platform (Adams et al., 2006, Kim et al., 2017). TiO<sub>2</sub>, especially as nanoparticulate anatase, is thought to be an interesting antibacterial agent with notable photocatalytic behavior (Krug., 2008). Also, the stability of NPs in solutions is important for the antimicrobial properties of NPs, specifically causing bacterial cell membrane damage (Kumari et al., 2014). While many studies have examined the antimicrobial properties of NPs in controlled lab environments against bacterial isolates, previous studies have also shown that NPs, such as TiO<sub>2</sub> NPs, caused a shift in microbial community structure and diversity in soil and stream environments (Battin et al., 2009, Moll et al., 2017, Ward et al., 2019). In addition, NPs have been shown to affect some of the bacteria that are responsible for the removal of nitrogen and phosphorus from the environment and cause a decrease in aquatic microbial diversity and change in the composition of microbial species (Liu et al., 2018, Ward et al., 2019, Londono et al., 2017). One study showed that the addition of Ag-NP changed microbial diversity and community composition compared to the controls where no Ag-NP were added (Ward et al., 2019). While there are fewer reports of bacterial resistance to nanoparticles compared to reports of biocide resistance, a recent study examined the potential for E. coli to develop resistance to Ag-NP. Panacek et al., (2018) demonstrated that after 20 transfers in the presence of Ag-NP, E. coli became more than 10 times more resistant to Ag-NP than the parental strain. The mechanism of enhanced resistance was shown to be related to the overexpression of flagellin proteins, which resulted in aggregation of Ag-NP leading to the enhanced tolerance of the Ag-NP. Few studies have directly compared the impact of biocides and NPs on natural microbial communities in the context of previous hydraulic fracturing contamination. Here, we sought to better understand the environmental effects of biocides and nanoparticles through comparing the

94

95

96

97

98

99

100

101

102

103

104

105

106

107

108

109

110

111

112

113

114

115

effects of biocides and NPs on microbial abundance and community composition. A microcosm-based approach was used, where stream water was treated with either biocides or NPs and changes in cytotoxicity measures, microbial abundance, and microbial community composition were tracked. Previous work has shown that biocides strongly and rapidly alter microbial community composition (Gilbert and McBain, 2003, Campa et al., 2019). Other studies have shown that Ag-NP can strongly impact microbial community composition. We hypothesized that biocides would result in more strongly altered microbial community composition relative to NPs.

# Materials and methods

(Table.1).

The biocides used in this study were 2, 2-dibromo-3-nitrilopropionamide (DBNPA) (molecular weight: 241.87 g/mol, Sigma-Aldrich), Triclosan (molecular weight: 289.54 g/mol, Sigma-Aldrich), and Glutaraldehyde (molecular weight: 100.12 g/mol, Sigma-Aldrich). Stock solutions of each were prepared at a concentration of 100 mg/L.

The nanoparticles used in this study were commercial preparations of metal oxide nanoparticles (US Research Nanomaterials, Inc. 3302 Twig Leaf Lane, Houston, TX 77084, USA). The nanomaterials were 99.9% TiO<sub>2</sub> with a diameter of 18 nm (Cat No. US3490), 99.95% ZnO with a diameter of 18 nm (Cat No. US3599) and 99.5% SiO<sub>2</sub> with a diameter of 18 nm(Cat No. US3436) all of the nanoparticles were spherical in shape. Molecular weight of TiO<sub>2</sub> is 79.87 g/mol. Molecular weight of ZnO is 81.38 g/mol. Molecular weight of SiO<sub>2</sub> is 60.08 g/mol

Table.1. Showing the chemicals as biocides or NPs used in this study

	Antimicrobial		
Antimicrobial	type	Chemical Structure	Chemical Formula
Glutaraldehyde (GA)	Biocide	H O O	C <sub>5</sub> H <sub>8</sub> O <sub>2</sub>

2, 2-dibromo-3- nitrilopropionamide (DBNPA)	Biocide	N NH <sub>2</sub>	C <sub>3</sub> H <sub>2</sub> Br <sub>2</sub> N <sub>2</sub> O
Triclosan (TCS)	Biocide		C <sub>12</sub> H <sub>2</sub> Cl <sub>3</sub> O <sub>2</sub>
Titanium oxide (TiO <sub>2</sub> )	Nanoparticles	0=Ti=0	TiO <sub>2</sub>
Zinc oxide (ZnO)	Nanoparticles	Zn=0	ZnO
Silicon dioxide (SiO <sub>2</sub> )	Nanoparticles	O=Si=O	SiO <sub>2</sub>

137

138

139

140

141

142

143

144

145

146

147

148

149

150

151

152

153

154

# Microcosm set up

Stock solutions of nanoparticles were prepared at a concentration of 100 mg/L in sterile Milli-Q water and sonicated in an ultrasonic bath (Sonicator) for 20-30 min and stored in a refrigerator and used within a week. Surface water was obtained from Lower Greys Run, PA. The water for culturing was collected in a sterile 500 mL plastic bottles and stored on ice (Fig.S1). The bottles were shipped on ice to Michigan Technological University on ice and stored at 4°C until microcosm set up after a week. Thirty mL of stream water were placed into sterile serum bottles in triplicate. One set of bottles was used as a control with no amendment. The controls were used to track the normal growth of the microbial cells without nanoparticles or biocides to understand the bottle effect. This condition served as a negative control to control for change in microbial community diversity and composition that resulted from factors other than treatment with antimicrobials. Other microcosms were set up where nanoparticles or biocides were added to the water samples. Five ml of the 100 mg/L stock of nanoparticles or biocides was added to 25 ml of stream water to make 16.7 mg/L as the final concentration. The working concentration for all treatments in molarity were as follows: 0.069 mM for DBNPA, 0.057 mM for triclosan, 0.166 mM for glutaraldehyde, 0.21 mM for TiO<sub>2</sub>, 0.21 mM for ZnO, and 0.28 mM for SiO<sub>2</sub>. Our experimental design controlled for gravimetric concentration. Previous studies into the impacts

of biocides or nanoparticles on microbial communities have used gravimetric concentrations (Campa et al., 2019, Campa et al., 2018, Ward et al., 2019). Therefore, controlling for gravimetric concentration allows for comparison with previous work. However, this design also enables us to test if higher molar concentrations of NP have stronger effects on microbial community diversity and composition. We chose these concentrations of biocides and nanoparticles based on previous studies that have shown that similar or lower concentrations of antimicrobials resulted in effects on the microbial community (Ward et al., 2019, Battin et al., 2009, Drury et al., 2013, Gnanadhas et al., 2013, Vikram et al., 2015a). All conditions were set up in triplicate. Time zero samples were collected after all microcosms were set up. The bottles were incubated aerobically at 25°C in the dark. Bottles were sacrificially sampled at the given time points. The water was filtered through a 0.2 µm pore size, polyethersulfone (PES) membrane with a 47 mm diameter using a vacuum pump. The filters were retained for DNA extraction. Time zero samples were collected after the addition of antimicrobials and after all of the microcosms were set up. Therefore, there were slight difference in the time from exposure to antimicrobials and sample collection for the time zero conditions. Filtered water was kept for the measurement of pH and LDH activity. Measurements were taken every 0, 1, 7, and 14 days.

### Nanoparticle characterization

155

156

157

158

159

160

161

162

163

164

165

166

167

168

169

170

171

172

173

174

175

176

177

The size and charge of nanoparticles in stream water were determined throughout the experiment. Size and zeta potential were determined using a Malvern zetasizer at 25°C. The zetasizer measures particle and molecular size using dynamic light scattering (DLS) and zeta potential and electrophoretic mobility using electrophoretic light scattering. The size distribution and charge of the nanoparticles were determined from the average of independent size (d. nm) measurements. The average size distribution was determined for each replicate. The size of the

nanoparticles was determined based on intensity. The average of the particle size distribution and zeta potential for most treatments were measured three independent times. TiO<sub>2</sub> day 0, ZnO day 0, SiO<sub>2</sub> day 0, TiO<sub>2</sub> day 7 are only shown as the average size distribution of three independent measurements on the zetasizer and reported as the average size distribution. For all other samples, each independent measurement is reported allowing for standard error and standard deviation to be reported (Table.S1 and Table.S2).

Nanoparticles were also characterized by Transmission Electron Microscopy (TEM) to confirm the studied particles size and shape. To perform TEM, we pipetted 5 µl from 16.7 mg/L of nanoparticles incubation bottles at day 0 on to a carbon-coated grid. Samples examined by TEM images using a FEI 200kV Titan Themis S-TEM microscope at an accelerating voltage of 80 kV (FEI company, USA). The specimens were prepared for each NPs in a closed tube.

### pH measurements

The pH of the microcosms was measured in order to determine the change in the pH of stream water as a result of treatment. The pH of a system can impact the microbial community composition (Hou et al., 2017). The pH measurements were taken for the filtered water every 0, 1, 7, and 14 days. The pH was measured using Fisherbrand<sup>TM</sup> accumet<sup>TM</sup> AB250 pH/ISE Benchtop. A Shapiro-Wilk test was used to determine if the pH data were normally distributed. Since the data were not normally distributed, a Kruskal-Wallis test was used to compare between time and treatments and evaluate the significance of the pH change relative to the control (P<0.05 was considered significant). Dunn's test was used as a post hoc test. For the Dunn test p-

values were corrected for multiple comparisons using a Benjamini-Hochberg false discovery rate correction.

201

202

203

204

205

206

207

208

209

210

211

212

213

214

215

216

217

218

219

220

199

200

### Membrane permeability assessment - lactate dehydrogenase assay (LDH)

Lactate dehydrogenase (LDH) measurements estimate the viability of bacterial cells by detecting the damage of bacterial cell membrane structure (Kumari et al., 2014). LDH is an intracellular enzyme. High concentration of LDH outside of the cell is an indication of cellular damage and cytotoxicity. LDH functions in the conversion of lactate to pyruvate by reducing the NAD+ to NADH and vice versa. The filtrate from each microcosm was saved and used to measure cytotoxicity. LDH was measured following standard protocols. LDH was measured as follows: 100 µL from each filtered water bottles were mixed with 30 mM sodium pyruvate, and 2.8 mL of 0.2 M Tris-HCl. Then 100 μL of 6.6 mM NADH were added to the mixtures. LDH activity was measured by tracking absorbance at 340 nm using a UV-vis spectrophotometer (Kumari et al., 2014). The LDH measurements were taken for the filtered water after 24hr. A Shapiro Wilk test was used to determine if the LDH data were normally distributed. The data were not normally distributed; therefore, a Kruskal-Wallis test was used to determine if there were significant differences between treatments at different times as well as if there were differences between nanoparticle or biocide conditions at different times. A Dunn test was used as a post hoc test to determine between which conditions and times were their significant differences. For the Dunn test p-values were corrected for multiple comparisons using a Benjamini-Hochberg false discovery rate correction.

## **DNA** extraction

DNA was extracted from the water filters using the Zymobiomics DNA extraction kit. Sterilized scissors and forceps were used to cut the 47 mm filters in half in a sterile petri dish. The Zymobiomics DNA extraction kit protocol was followed according to the manufacturer's specifications (D4301, Zymo Research Corporation, Irvine, CA USA).

# **Bacterial abundance analysis (qPCR)**

221

222

223

224

225

226

227

228

229

230

231

232

233

234

235

236

237

238

239

240

241

242

243

Abundance of the 16S rRNA gene was determined using quantitative Polymerase Chain Reaction (qPCR) quantifying the abundance of the 16S rRNA gene. We used gene copies of the 16S rRNA gene as a proxy for microbial abundance. qPCR was performed as previously described in (Techtman et al., 2017). The qPCR reaction set up as follows: 10µl of SYBR® Green RT-PCR master mix, 0.5 µl of each primer (20 µM) Bact341F and Uni519R primers (Jorgensen et al., 2012), 2 µl of Environmental DNA, and 7 µl Sterile nuclease- free water. Reactions were prepared in white 96 well PCR plates that have been sterilized by autoclaving. The amplification was carried out in a StepOnePlus<sup>TM</sup> Real-Time PCR System thermocycler (Thermos Fisher Scientific Waltham, MA USA). The following temperature protocol was used: 95°C for 15 min and 35 cycles of 95°C for 15 sec, 58°C for 30 sec, and 72° C for 30 sec. The CT values or threshold cycle is the cycle number at which the fluorescence generated within a reaction crosses the fluorescence threshold, which provides the amount of the gene amplicon product were converted to a number of copies using a standard curve based on the standards described in (Techtman et al., 2017). The concentration values were converted to logCT and  $\log(\text{copies})$  and followed the equation y = -11.932x + 20.312 with an  $R^2$  of 0.9594 for our standard curve. The data obtained in all tests were compared with the control. A Shapiro-Wilk test for normality was used to determine if the qPCR gene copies data were normally distributed. The data were not normally distributed, so a Kruskal-Wallis Test was used to evaluate the

significance of experimental results (P<0.05). A Dunn's test was used as a post hoc to evaluate the significance of experimental results (P<0.05). Comparisons were performed between treatments and the control as well as to see if there were significant differences between biocideand NP-amended treatments and the control.

# Microbial community composition analysis (16S rRNA) gene sequencing

244

245

246

247

248

249

250

251

252

253

254

255

256

257

258

259

260

261

262

263

264

265

The microbial community composition profile was determined using 16S rRNA gene sequencing of the environmental DNA. The 16S rRNA gene was amplified to profile changes in taxonomic diversity in these microcosms. The PCR reactions were set up using Phusion® High-Fidelity PCR Master Mix (Thermo Fisher Scientific, Waltham, MA, USA), and 515YF and 926R primers at a concentration of 0.4 µM to amplify V4-V5 region (Parada et al., 2016). The amplification was carried out in a thermocycler with the following protocol: 95 °C for 3 min, 25 cycles of 95 °C for 30 sec, 55 °C for 30 sec, 72 °C for 30 sec, followed by one cycle of 72 °C for 5 min. PCR clean-up was done on the initial amplicon. Following the Illumina MiSeq 16S rRNA metagenomic library prep guides (Illumina, San Diego, CA), AxyPrep MAG PCR clean-up beads (Corning, Big Flags, NY, USA) were used for the PCR cleanup process. The final product was eluted in 25 µL 10mM Tris buffer at pH of 8. Sequencing adapters were added with a second PCR where 5 µl were added from the first PCR reaction and different index forward and reverse primers were added to each reaction then performed an 8 cycle PCR. The indexed PCR product was purified using the AxyPrep MAG PCR clean-up beads. Finally, 16S rRNA gene sequencing was done using the Illumina MiSeq (Illumina, SanDiego, CA). The concentration of each of the cleaned 16S rRNA PCR reactions was determined using PicoGreen<sup>TM</sup> (Thermo Fisher Scientific, Waltham, MA, USA). We pooled all our samples with the same concentration

in to one pool and diluted the pool to 1.5 nM. Then we followed the MiSeq v2 600 cycle kit (2 x 300) protocol. Raw reads are deposited at the SRA (BioProject accession PRJNA663853). All data analysis was performed in R. Raw sequencing reads were demultiplexed by the Illumina MiSeq platform. The DADA2 package was used to remove primer nucleotides, merge pairedend-reads, filter by quality, and remove internal standard phiX. To account for true biological variation within our samples, DADA2 was used to infer ASVs (amplicon sequence variants) and remove chimeric sequences through a Needleman-Wunsch global alignment. From 408549 paired-end input reads, 403744 nonchimeric reads passed filtering parameters and were used as ASVs for analysis in this study. Taxonomy of ASVs was assigned through DADA2 with a rapid assignment naive Bayesian classifier using the SILVA v132 training set (Callahan et al., 2016). Only samples with more than 1000 reads were used in downstream analyses. Due to low sequencing yields, this resulted in a substantial number of treatments being removed from the dataset. Therefore, we compared the microbial community composition for each treatment on day 0 and 14 of the experiment to analyze the impact of treatment on microbial community composition. For day 0 only the control, triclosan, TiO<sub>2</sub>, ZnO, and SiO<sub>2</sub> treatments had more than 1000 reads after quality filtering and were included in our analysis. Diversity analyses were performed using phyloseq (McMurdie and Holmes, 2013). Alpha diversity was determined through rarifying the ASV table 100 times to the lowest number of sequences per sample (1111 reads). Shannon diversity, Inverse Simpson, and Observed ASVs were determined for each of the 100 tables. The average diversity for the 100 tables was calculated. A Shapiro-Wilk test was used to determine if the data was normally distributed. All three metrics were normally distributed so an ANOVA was used to assess significance in the diversity between Nanoparticles and Biocides at day 14.

266

267

268

269

270

271

272

273

274

275

276

277

278

279

280

281

282

283

284

285

286

287

To assess differences in microbial community composition, we performed a Principal Coordinate Analysis (PCoA) based on a Bray Curtis dissimilarity matrix from an ASV table rarified to 1111 sequences per sample. To determine if there were significant differences in the microbial community composition between nanoparticles and biocide treatments, a PERMANOVA of Bray Curtis dissimilarity was run using the adonis2 program in the vegan package in R. Differential abundance was performed using DESeq2 (Love et al., 2014) to identify ASVs that were enriched in either the NP or biocide treatments at day 14. ASVs were considered enriched if they had a log2 fold change in abundance of greater than 2 and an adjusted p valued of < 0.05.

### Results

### Metal oxide nanoparticles size and stability

To study the stability of NPs at a concentration of 16.7 mg/L in the stream water and their aggregation behavior, the size and zeta potential were measured at different days (0, 1, 7, and 14 days) (Table. 2, Table.S1, and Table.S2). Throughout the experiment, the mean of the size distribution of TiO<sub>2</sub> NPs decreased in size from 667.6 nm at day 0 to 280.13 nm at day 14. Similarly, the mean of the size distribution of the ZnO NPs decreased in size from 397.7 nm at day 0 to 280.13 nm at day 14. With SiO<sub>2</sub> NPs there was an increase in mean of the size distribution from 387.9 nm at day 0 to 548.63 nm at day 14. Zeta potential has been used as an indicator of dispersion stability. With all NPs, the zeta-potentials were highly negative, which suggests that they are stable in the water samples. The zeta potentials were less than -18.7 mV which represents the dispersion of particles. The size of the NPs in the 16.7 mg/L solutions of the three nanoparticles and stream water was also measured using TEM (Fig.1).

Table.2. Showing the mean size distribution, zeta potential, and their standard error in Lower Grays water treated samples over time (n=3) (average  $\pm$  standard error).

Type of Nanoparticles		TiO <sub>2</sub>		SiO <sub>2</sub>		ZnO	
Days	Size	Zeta	Size	Zeta	Size	Zeta	
-		Potential		Potential		Potential	
	(d. nm)	(mV)	(d. nm)	(mV)	(d. nm)	(mV)	
Day 0	667.6	-23	$387.9 \pm 5.8$	-18.1	397.7	-25.2	
Day 1	$457.9 \pm 0$	$-24.67 \pm 0.32$	$541.4 \pm 37.8$	-21.5 ± 1.2	$343.2 \pm 1.7$	-21.3 ± 1.2	
Day 7	269.9	$-18.7 \pm 0.76$	$460.83 \pm 20.9$	-28.8 ± 1.9	$203.76 \pm 3$	-27.3 ±2.9	
Day 14	$280.13 \pm 5.1$	$-24.03 \pm 0.9$	548.63 ±16.1	-24.3 ± 2.2	$280.13 \pm 15.7$	-18 ±1.8	



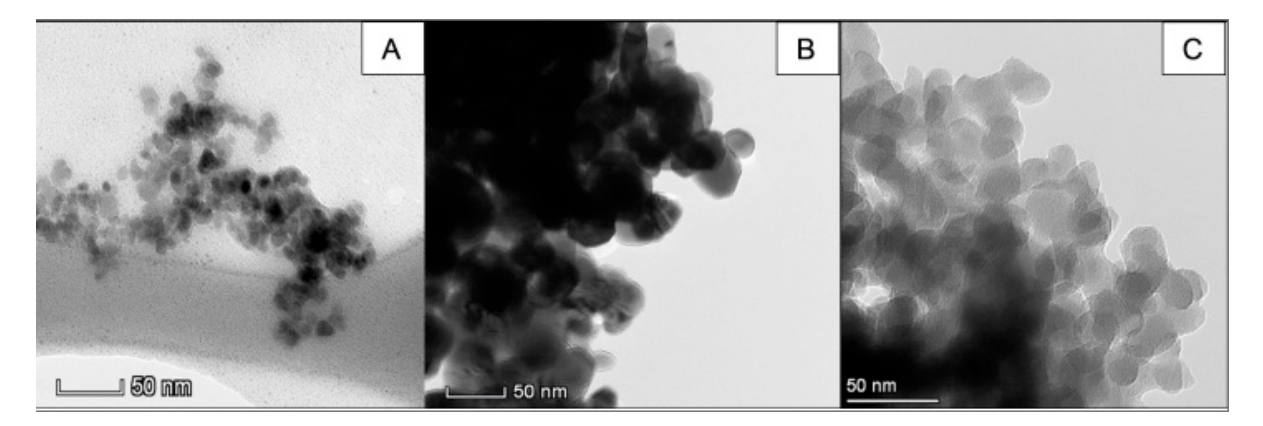


Fig. 1. Transmission electron microscopy photomicrograph of (A)  $TiO_2NPs$  stock solution, (B) ZnO NPs stock solution, (C)  $SiO_2NPs$ . stock solution Scale bars = 50 nm

### Change in pH over time and treatment

There was a significant difference in the pH in the NPs and biocide treatments and different times (Kruskal Wallis test p-value = 1.654 x 10<sup>-08</sup>) (Fig.S2, Table.S3, and Table S4). Despite the overall significant difference, there were only slight changes in the pH. When comparing the pH at time 0 and Day 7, significant differences were seen for SiO<sub>2</sub> (Dunn test adjusted p-value = 0.019) and Triclosan (Dunn test adjusted p-value = 0.015). When comparing the pH between Day 0 and Day 14, triclosan showed a significant difference (Dunn test p-value = 0.021) (Table.S4). In general, the pH level of the metal oxides NPs looked similar the control. On the other hand, biocides tended to lower the pH, especially with glutaraldehyde.

# Cytotoxicity effects of biocides and nanoparticles on bacterial membrane permeability (LDH)

LDH measurements were obtained from filtrate after 24 hours of incubation by measuring an OD340 using the filtered water for both NPs, biocides and the control samples (Fig.2). TiO<sub>2</sub> was the only treatment to give a higher LDH level than the control. No significant differences were observed for any of the treatments in comparison to the control on day 1. The LDH level for triclosan, glutaraldehyde, DBNPA, ZnO, and SiO<sub>2</sub> were all less than the control at 24 hours.

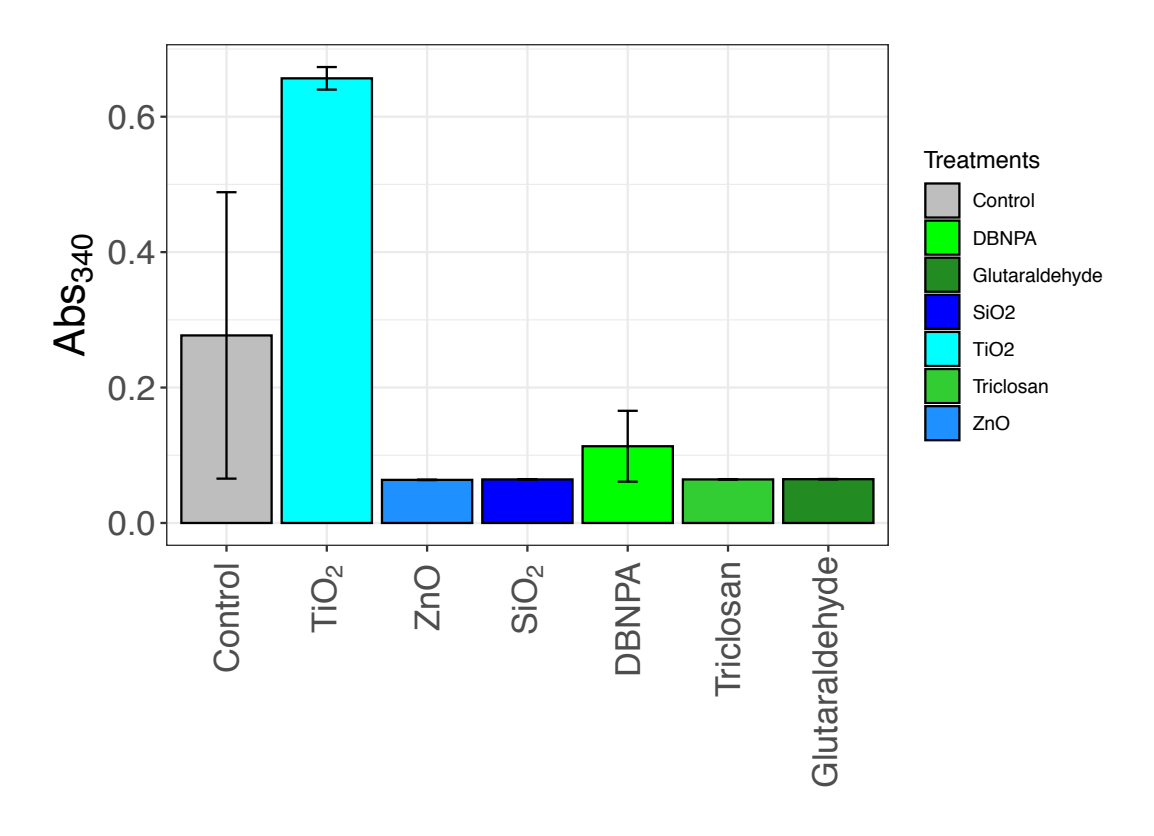


Fig.2. LDH activity for microcosms treated with 16.7 mg/L concentration of biocides and NPs after 24h incubation and the standard error (n=3).

# Effect of NPs and biocides on 16S rRNA gene copies

The change of the 16S rRNA gene abundance was determined by using qPCR (Fig.3 and Table.S7). We used the copies of the 16S rRNA gene as a proxy for bacterial abundance changes

with different treatments. To understand that impact of treatments on microbial abundance, we compared the microbial abundance between treatments and the control across the time series as well as comparing the microbial abundance at later time points compared to the initial time point. Overall, between day 0 and day 14, there was an increase in microbial abundance in the biocide treatments (Figure 3). On the other hand, the microbial abundance in NPs treatments looked similar to the control as it decreased over time. However, the bacterial abundance in GAamended microcosms had the greatest change in number of copies from  $8.54 \times 10^3 \ (\pm 1.53 \times 10^3)$ copies/ml at day 0 to 2.99 x  $10^7$  ( $\pm 9.97$  x  $10^6$ ) copies/ml at to day 14. For the biocides the DBNPA treatments showed the least change in abundance over the experiment with a change of 7.48 x 10<sup>3</sup> to 1.29 x 10<sup>5</sup> copies/ml between day 0 and day 14. The Triclosan treatments showed the least change in abundance over the experiment with a change of  $1.18 \times 10^4$  to  $1.12 \times 10^8$ copies/ml between day 0 and day 14. The biocides treatments on average increased by 2.7 log from day 0 to day 14. The increase microbial abundance was significant between day 0 and day 14 (Kruskal Wallis chi-squared = 42.4643, degrees of freedom = 11, p-value = 0 and Dunn Test adjusted p value 0.0029). In contrast, the bacterial abundance of the nanoparticle treatment decreased over time. For example, the SiO<sub>2</sub> treatments decreased from 1.02 x 10<sup>7</sup> to 5.43 x 10<sup>4</sup> copies/ml from day 0 to day 14. 16S rRNA gene copies in the TiO<sub>2</sub> decreased from 2.29 x 10<sup>6</sup> copies/ml on day 0 to 1.41 x 10<sup>4</sup> copies/ml on day 14. Finally, ZnO treated microcosms had the largest decrease in the number of copies of the 16S rRNA gene over the experiment from 3.94 x 10<sup>7</sup> copies/ml to 2.81 x 10<sup>4</sup> copies/ml. The nanoparticle treatments on average decreased by 2.8 log from day 0 to day 14. When taken together the Nanoparticle treatments showed a significant decrease in the 16S

338

339

340

341

342

343

344

345

346

347

348

349

350

351

352

353

354

355

356

357

358

rRNA gene copies per ml between day 0 and day 14 (Kruskal Wallis chi-squared = 42.4643, degrees of freedom = 11, p-value = 0 and Dunn Test adjusted p value 0.0038)

In general, the gene copies at time zero for the biocide treatments were significantly lower than the gene copies for time zero for the control and nanoparticles (Dunn test adjusted p-value of Biocides vs control (0.0028) Dunn test adjusted p-value of Biocides vs Nanoparticles (0.0007). This difference may be due to the activity of the biocides during the time from the addition of the antimicrobials to when the samples were filtered. The significant increase of microbial abundance in biocide treatments over time might suggest the presence of resistant bacteria in

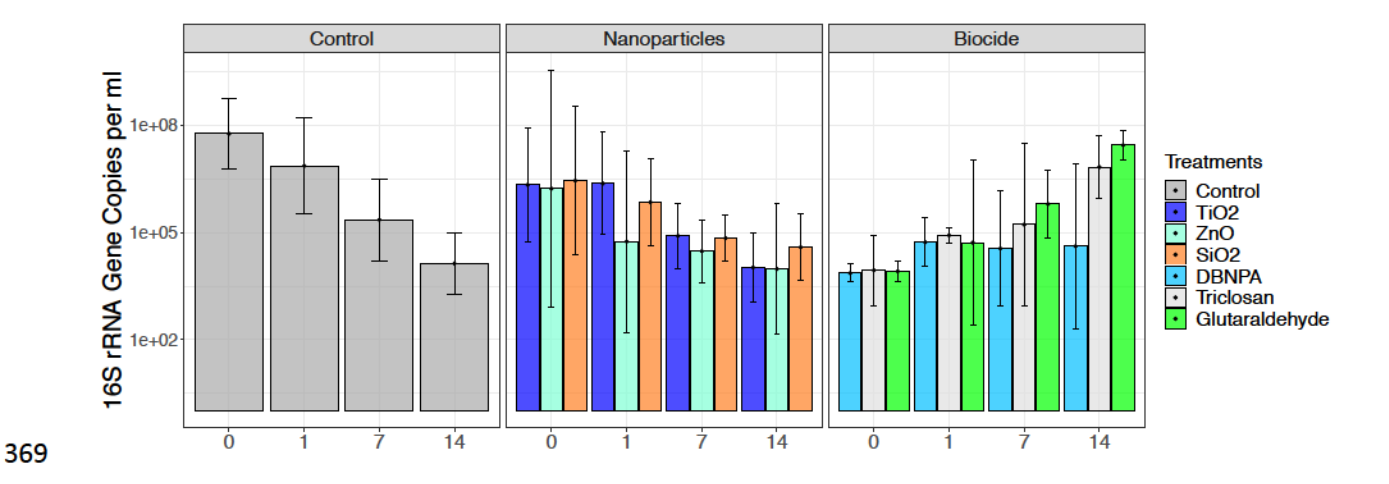


Fig.3. Changes in microbial abundance over time. The mean and standard deviation of 16S rRNA gene copies for each timepoint of nanoparticles and biocides microcosms from in Lower Grays Run, PA samples.

### Microbial community structure

these streams.

## Changes in alpha diversity in biocide and nanoparticle treatments.

Overall NP microcosms had higher evenness and richness than biocide treatments after 14 days of incubation. On day 0, the control, all three nanoparticle treatments, and the triclosan treatment all had similar alpha diversity. After incubation, the triclosan and glutaraldehyde treatments had

lower diversity than the control and nanoparticle treatments. The DBNPA treatment at 14 days had high Shannon diversity, Inverse Simpson's diversity, and Observed ASVs, which were similar to the control and the nanoparticle treatments. When comparing the diversity of biocide treatments with NPs and control at day 14, there were no significant differences between biocides and NP for any of the three alpha diversity metrics tested. (ANOVA p-values Shannon: 0.657, Inverse Simpson: 0.898, and Observed ASVs: 0.624) (Supplemental Table.S10).

### Principal coordinate analysis (PCoA):

378

379

380

381

382

383

384

385

386

387

388

389

390

391

392

393

394

395

396

397

398

399

PCoA analysis of a Bray Curtis dissimilarity matrix from the rarified ASV table showed three distinct groups (1) the initial time points, (2) triclosan and Glutaraldehyde at day 14 and (3) NPs, and control at day 14 (Fig.4). The PCoA analysis shows that all of the nanoparticles, the control, and triclosan (the only one of the initial biocide treatments to have sufficient sequences) clustered together at time zero. This indicates that the microbial community composition of the starting communities was similar despite the initial difference in microbial abundances. After 14 days of incubation, a divergence in community composition was observed between the triclosan and glutaraldehyde compared to the NPs and the control. On day 14, the three nanoparticles and the control clustered together, whereas the biocide treatments were distant from the control and from each other. This finding suggested there was a change in the microbial community between biocide and NPs samples, which indicate that biocides alter the microbial community composition more strongly than the nanoparticles. Interestingly the DBNPA treatment at day 14 clustered more similarly to the initial time points. This could be in part due to the short half-life of DBNPA and water (Campa et al., 2019). Permutational multivariate analysis of variance (PERMANOVA) was used to test the hypothesis that the microbial community composition in

the biocide treatments on day 14 was significantly different from the nanoparticle treatments at different time points (PERMANOVA P-value 0.009, degrees of freedom 5, R<sup>2</sup> 0.613).

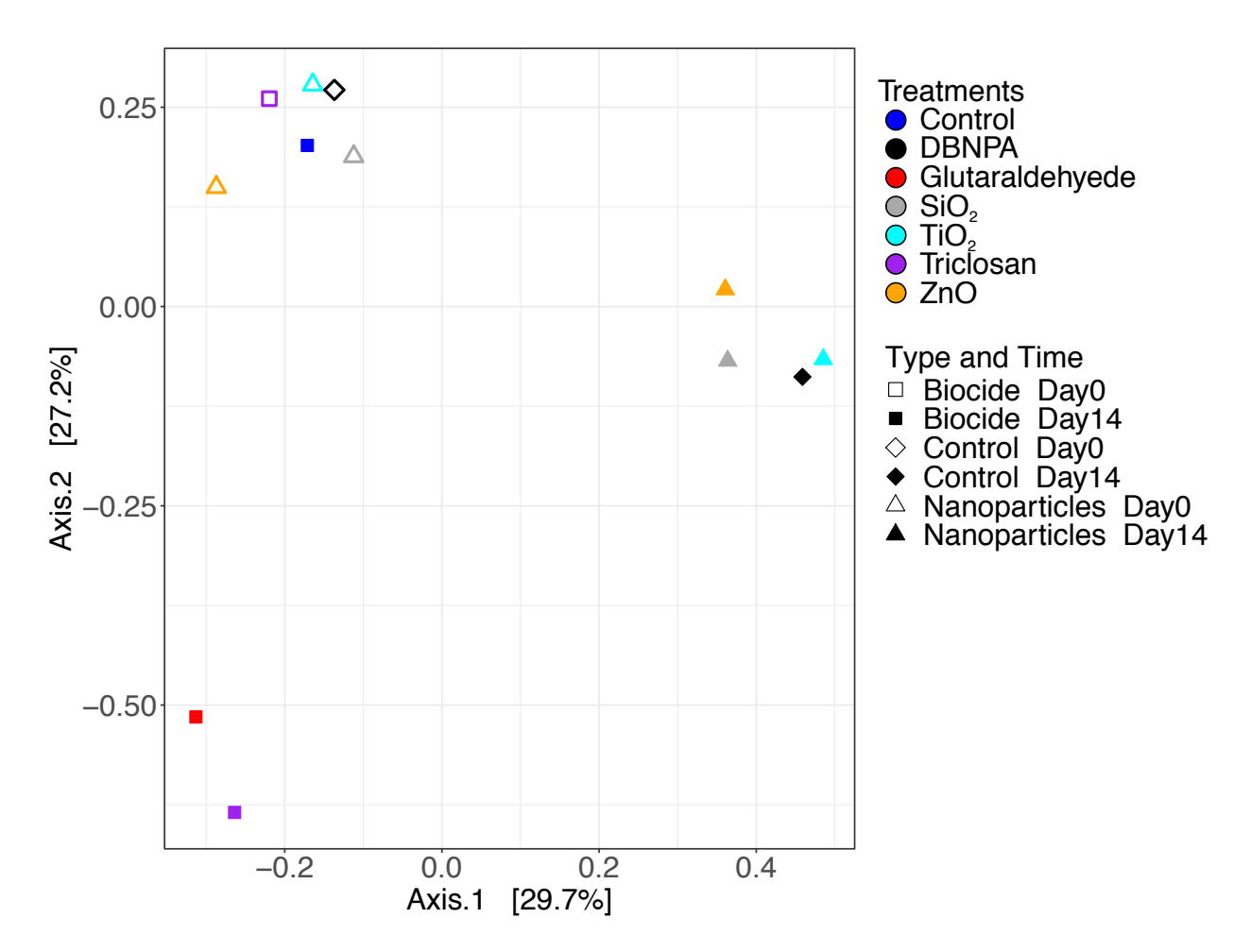


Fig.4. Principal coordinate analysis (PCoA) of Bray Curtis Dissimilarity of the rarified ASV table of microcosms from Lower Grays Run, PA samples with 16.7 mg/L concentration of three metal oxides NPs and biocides. This is showing the dissimilarity of the microbial community on day 0 (open symbols) and day 14 (closed symbols). Treatments are shown as different colors

### Differentially enriched taxa between NPs and biocides microcosm:

To better understand which taxa were differentially abundant in the different treatments, we analyzed the community composition of each treatment at the taxonomic level of order. The change in the taxonomic diversity measured by the relative abundance in each taxonomic order for all treatments is shown in (Fig.5). At initial time points, the communities in all samples were

relatively similar. The communities had high levels of Betaproteobacteria, Pseudomonadales, Flavobacteriales, and Cytophagales. After 14 days, there were changes in the taxonomic composition of all treatments. In the control, the initial bacterial population was primarily Betaproteobacteriales with Chitinophageles as the second most abundant order, and Salinisphaerales was the third most abundant. Similar trends were observed in the three NPs. The Cytophagales showed higher relative abundance with SiO<sub>2</sub> NPs treatment than the control. The population of Sphingomonadales in SiO<sub>2</sub> NPs treatments was also higher than the other NPs. On the other hand, in the SiO<sub>2</sub> treatments, there was a reduction in the Betaproteobacteriales abundance compared to the control and NPs microcosms. Pseudomonadales were dominant members of the microbial community in the triclosan and glutaraldehyde treatments. The second most abundant group in the three biocide microcosms were Xanthomonadales. Despite the short half-life of DBNPA (63 hours at a pH of 7) (EPA, 2012), there was a distinct microbial community composition in the DBNPA treated microcosms with members of the Cytophagales and the Flavobacteriales being more abundant compared to the control and other biocide treatments. We performed differential abundance analysis using DESeq2 on day 14 samples to identify the differentially abundant taxa between biocides and nanoparticles. Fifteen ASVs were determined to be significantly enriched in either the nanoparticles or the biocide treatments (Table.S11). Twelve ASVs were significantly enriched in the biocide treatments, and eight ASVs were enriched in the nanoparticle treatments. Five of the ASVs enriched in the biocide treatments were annotated as Pseudomonadales. Two of the ASVs enriched in the biocide were annotated as Xanthamonadales. The remaining five ASVs were annotated as members of the Burkholderiaceae (Delftia, Janthinobacterium, and Herbaspirillum) and Rhodanobacteraceae

412

413

414

415

416

417

418

419

420

421

422

423

424

425

426

427

428

429

430

431

432

433

(Luteibacter and Dyella). The five ASVs enriched in the nanoparticle treatments were members of the Burkholderiaceae, Sphingomonadaceae, and Methylophilaceae. These findings confirm the overall observations from the taxa plots (Fig.5).

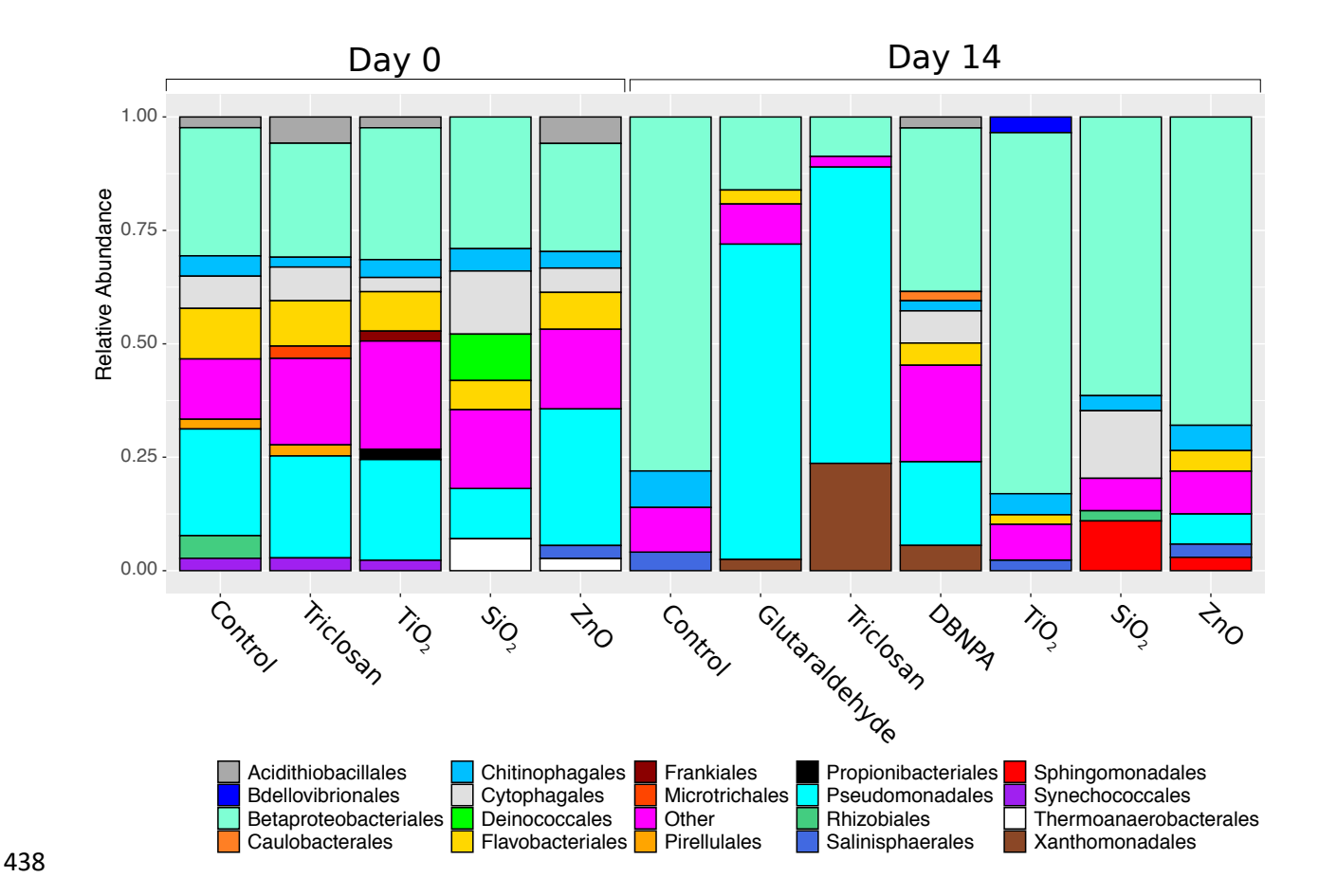


Fig. 5: Bar graph of taxonomic diversity shows the relative abundance of bacterial order with those classes represented with different colors. This figure shows the relative abundance of bacterial orders on day 0 and day 14 for Lower Grays Run, PA samples incubated with three metal oxide nanoparticles, and biocides at 16.7 mg/L concentration for all treatments.

# **Discussion**

The objective of this study was to compare the impact of biocide and NPs on natural microbial communities in a hydraulic fracturing impacted stream. Our hypothesis was that biocides will result in a more strongly altered microbial community composition relative to NPs.

# Stability of NPs in stream water

The characteristics of metal oxide NPs in water are shown in table.1. While TEM images of the NPs stock suspension showed similar size to the commercial reported values (Fig.1), the average size distribution of the nanoparticles, were much larger than reported size with average size from 203.7–667.6. This finding suggests that the NPs aggregated in water due to having diameters larger than 100 nm size. This aggregation of NPs may decrease the antimicrobial efficacy (Slavin et al., 2017). However, this trend of NPs aggregating in natural water is similar to what has been observed previously, where researchers observed larger metal oxide nanoparticles size with 200-800 nm range than the commercial size when they add them to water samples (Zhang et al., 2008). The zeta potential of all metal oxide NPs in water samples were negative.

### The change in pH of microcosms as a result of treatment

On day 0 and day 14, glutaraldehyde (GA) had the lowest pH level of all of the treatments  $(4.9\pm0.02 \text{ to } 6.1\pm0.2)$ , which indicates more acidic conditions in this treatment. Previous studies have found a similar change in pH in GA amended microcosms (Campa et al., 2018). Glutaraldehyde can be biodegraded under aerobic conditions to glutaric acid, which could affect the pH of these microcosms.

### The cytotoxicity of NPs & biocides

The NPs were selected in this study due to their antibacterial properties (Kadiyala et al., 2018). Previous work demonstrated that concentrations of TiO<sub>2</sub> as low as 5.3 mg/L had an effect on microbial communities (Battin et al., 2009). Additionally, Ag NPs were shown to be effective at concentrations as low as 10 mg/L (Ward et al., 2019). Our results show that TiO<sub>2</sub> NPs had the highest cytotoxic effect compared to other NPs and biocides based on high levels of LDH

activity at 24 hours in the TiO<sub>2</sub> treatments. It has previously been reported that some NPs target the membrane of some bacteria conferring the antimicrobial properties of NPs (Bondarenko et al., 2018). In particular, TiO<sub>2</sub> has been shown to cause membrane damage to cell (Joost et al., 2015). Therefore, we expected that some NPs would result in increased LDH activity due to destabilizing of membranes, which would result in releases of LDH. TiO<sub>2</sub> NPs are known for their UV-induced antimicrobial activity (Ripolles-Avila et al., 2019). It was surprising to see such antimicrobial activity for TiO<sub>2</sub>, especially under dark conditions. However, previous work has shown that TiO<sub>2</sub> can generate radicals in the dark (Kumari et al., 2014). Therefore, this high LDH activity could be due to non-UV radical generation. This activity could damage the cell membrane and increased the permeability of the bacterial cell membrane and cell death. The 16s rRNA gene abundance results showed that between day 0 to day 14 there was increases in microbial abundance in each of the biocide treatments. Conversely, microbial abundance decreased from day 0 to day 14 in the NP-treated samples as well as the control. This increase in microbial abundance over time in biocide treated samples is similar to previous reports of increased gene copies in later time points of glutaraldehyde amended microcosms (Campa et al., 2018). This increase in gene copies may suggest the ability of biocides to select for resistant bacteria. Alternatively, the increase in microbial abundance may also be due to microbes utilizing the biocides as a carbon source. However, for a microbe to metabolize a biocide, it must be resistant to the biocide. We saw the highest change in bacterial abundance within glutaraldehyde treated microcosms. Previous work showed that cell abundance increased at later time points in GA amended microcosms from other hydraulic fracturing impacted streams (Campa et al. 2018). This increase in cell abundance was attributed to the biodegradation of GA and the increase of glutaric acid (Campa et al., 2018). The increase of glutaric acid reported in

469

470

471

472

473

474

475

476

477

478

479

480

481

482

483

484

485

486

487

488

489

490

the previous study started after day 7. In contrast to the results for the biocide-amended treatments, the microbial abundance of NP treated samples showed similar trends to the control microcosms of decreasing microbial abundance over time.

# The effects of NPs & biocides on bacterial community composition and diversity

492

493

494

495

496

497

498

499

500

501

502

503

504

505

506

507

508

509

510

511

512

513

Alpha diversity analysis indicated there was a change in the richness and evenness of the communities within some of the biocide microcosms after 14 days compared to NP microcosms, which were similar to the control as well as the initial conditions. Shannon diversity showed decreases in evenness and richness in glutaraldehyde and triclosan treatments compared to the others. Campa et al 2018 found that addition of GA resulted in a decrease in diversity. The extent of the decrease in diversity was affected by previous contamination state. Streams impacted by HF often showed less of a decrease in diversity in response to GA addition. Our results that GA and triclosan result in a decrease in diversity matches their results. Our results also demonstrated a strong impact of biocide addition on microbial community composition. In our study we observed dramatically altered microbial community composition in biocide-amended microcosms. In particular, Pseudomonadales were enriched in the presence of both GA and TCS compared to time zero, the controls, and other NP treatments. This enrichment of Pseudomonadales could be due to some Pseudomonadales having resistance to biocides A recent study demonstrated that Pseudomonas aeruginosa and Pseudomonas fluorescens employ efflux pumps to resist glutaraldehyde (Vikram et al., 2015b). Additionally, another study had suggested the mechanisms of resistance to TCS by using efflux pumps (Carey and McNamara, 2014). It is possible that the Pseudomonadales in these streams are employing mechanisms such as efflux pumps to survive biocide treatments.

Nanoparticle treatments showed increases in both Cytophagales and Sphingomonadales. This finding is in line with previous studies on the impact of pulsed addition of Ag NP on wetland microbial communities. In Ward et al 2019, they found that the addition of Ag NP resulted in increases in members of the Cytophagales after the first few days (Ward et al., 2019). Ward et al (2019) found that a member of the Cytophagales, *Flectobacillus*, dominated the pulsed treatments after the first few days. *Sphingomonas* were also found to be one of the key indicator organisms of Ag-NP addition. Ag NP have distinct properties from the metal oxide nanoparticles used in this study. These findings suggest that there may be common taxa that are resistant to NP in aquatic environments.

Hydraulic fracturing activity is a critical issue for environmental and public health and can present risks for ground and surface water contamination. Previous work has demonstrated that hydraulic fracturing activity can affect the response of stream communities to biocide exposure. Nanoparticles are an appealing alternative antimicrobial. Our results demonstrate a dramatic decrease in bacterial abundance with different types of nanoparticles. Conversely, microbial abundance increased for all of the biocide treatments over time. This may suggest the presence of biocide resistant bacteria in these streams as well as the ability of some taxa to use the biocides as a carbon source. Biocides strongly impacted the microbial community composition of freshwater. We observed changes in microbial taxa in response to antimicrobial additions that were similar to previous studies in other systems, suggesting some common microbial responses to antimicrobials in aquatic settings. Here we investigated NPs that are potentially more "environmentally friendly" than the commonly used antimicrobial silver NPs. While, there are some concerns about the risk of nanoparticle release into the environment, here we demonstrate

537	that the NPs chosen in our study have minimal effect on the microbial community. Our results
538	support the idea that nanoparticles may be a promising antimicrobial for diverse industrial
539	applications.
540	Acknowledgements
541 542 543	This work was funded by the National Science Foundation CBET awards 1804685 (Michigan Technological University), 1805152 (University of Tennessee), and 1805549 (Juniata College).
544 545 546 547	<b>Funding:</b> This work was funded by the National Science Foundation CBET awards 1804685 (Michigan Technological University), 1805152 (University of Tennessee), and 1805549 (Juniata College).
548 549	Conflict of Interest: All authors declare that they have no conflict of interest.
550 551	<b>Ethical approval:</b> This article does not contain any studies with human participants or animals performed by any of the authors."
552	<b>Author Contribution Statement</b>
553 554 555 556 557	RKA performed experiments, analyzed data and wrote the manuscript, RBG analyzed data and edited the manuscript, JRCS collected samples and edited the manuscript, OGW collected samples, MFC assisted manuscript preparation and edited the manuscript, TCH oversaw part of the analysis, RL oversaw sample collection, SMT assisted in experimental design, analyzed data and wrote the manuscript.
558	Data Availability
559	Raw 16S rRNA sequencing files have been deposited at NCBI under Bioproject PRJNA663853
560	

- ADAMS, L. K., LYON, D. Y. & ALVAREZ, P. J. 2006. Comparative eco-toxicity of nanoscale TiO2, SiO2, and ZnO water suspensions. *Water Res*, 40, 3527-32.
- AHAMED, M. I., INAMUDDIN, LUTFULLAH, SHARMA, G., KHAN, A. & ASIRI, A. M. 2016.
   Turmeric/polyvinyl alcohol Th(IV) phosphate electrospun fibers: Synthesis, characterization and
   antimicrobial studies. *Journal of the Taiwan Institute of Chemical Engineers*, 68, 407-414.
  - BATTIN, T. J., KAMMER, F. V., WEILHARTNER, A., OTTOFUELLING, S. & HOFMANN, T. 2009.

    Nanostructured TiO2: transport behavior and effects on aquatic microbial communities under environmental conditions. *Environ Sci Technol*, 43, 8098-104.
  - BONDARENKO, O. M., SIHTMÄE, M., KUZMIČIOVA, J., RAGELIENĖ, L., KAHRU, A. & DAUGELAVIČIUS, R. 2018. Plasma membrane is the target of rapid antibacterial action of silver nanoparticles in Escherichia coli and Pseudomonas aeruginosa. *International journal of nanomedicine*, 13, 6779-6790.
  - CALLAHAN, B. J., MCMURDIE, P. J., ROSEN, M. J., HAN, A. W., JOHNSON, A. J. & HOLMES, S. P. 2016. DADA2: High-resolution sample inference from Illumina amplicon data. *Nat Methods*, 13, 581-3.
    - CAMPA, M. F., TECHTMANN, S. M., GIBSON, C. M., ZHU, X., PATTERSON, M., GARCIA DE MATOS AMARAL, A., ULRICH, N., CAMPAGNA, S. R., GRANT, C. J., LAMENDELLA, R. & HAZEN, T. C. 2018. Impacts of Glutaraldehyde on Microbial Community Structure and Degradation Potential in Streams Impacted by Hydraulic Fracturing. *Environ Sci Technol*, 52, 5989-5999.
- CAMPA, M. F., TECHTMANN, S. M., LADD, M. P., YAN, J., PATTERSON, M., GARCIA DE MATOS AMARAL,
   A., CARTER, K. E., ULRICH, N., GRANT, C. J., HETTICH, R. L., LAMENDELLA, R. & HAZEN, T. C. 2019.
   Surface Water Microbial Community Response to the Biocide 2,2-Dibromo-3 Nitrilopropionamide, Used in Unconventional Oil and Gas Extraction. *Appl Environ Microbiol*, 85, 01336-19.
  - CAMPA, M. F., WOLFE, A. K., TECHTMANN, S. M., HARIK, A. M. & HAZEN, T. C. 2019c. Unconventional Oil and Gas Energy Systems: An Unidentified Hotspot of Antimicrobial Resistance? *Front Microbiol*, 10, 2392.
  - CAREY, D. E. & MCNAMARA, P. J. 2014. The impact of triclosan on the spread of antibiotic resistance in the environment. *Front Microbiol*, 5, 780.
  - CHATTOPADHYAY, S., HUNT, C. D., RODGERS, P. J., SWIECICHOWSKI, A. L. & WISNESKI, C. L. 2004. Evaluation of biocides for potential treatment of ballast water. BATTELLE MEMORIAL INST COLUMBUS OH.
  - DRURY, B., SCOTT, J., ROSI-MARSHALL, E. J. & KELLY, J. J. 2013. Triclosan exposure increases triclosan resistance and influences taxonomic composition of benthic bacterial communities. *Environ Sci Technol*, 47, 8923-30.
- 596 EPA 2012. Reregistration Eligibility Decision (RED) 2,2-dibromo-3-nitrilopropionamide (DBNPA). *Archived* 597 *from the original* Retrieved 2012-06-14., p. 179. .
  - FERNANDO, S. S. N., GUNASEKARA, T. & HOLTON, J. 2018a. Antimicrobial Nanoparticles: applications and mechanisms of action. *Sri Lankan Journal of Infectious Diseases*, 8, 2.
- FERNANDO, S. S. N., GUNASEKARA, T. & HOLTON, J. 2018b. Antimicrobial Nanoparticles: applications and mechanisms of action. *Sri Lankan Journal of Infectious Diseases*, 8, 2-11.
- 602 FINK, J. K. 2013. *Hydraulic Fracturing Chemicals and Fluids Technology*.
  - GILBERT, P. & MCBAIN, A. J. 2003. Potential impact of increased use of biocides in consumer products on prevalence of antibiotic resistance. *Clinical microbiology reviews*, 16, 189-208.
- 605 GNANADHAS, D. P., MARATHE, S. A. & CHAKRAVORTTY, D. 2013. Biocides--resistance, cross-resistance 606 mechanisms and assessment. *Expert Opin Investig Drugs*, 22, 191-206.

607 GRANT, D. M. & BOTT, T. R. 2005. Biocide dosing strategies for biofilm control. Heat Transfer 608 Engineering, 26, 44-50.

618

619

620

621

622

623

624

625

626 627

628

629

631

632

633

634

635

636

637

- 609 GUARDIOLA, F. A., CUESTA, A., MESEGUER, J. & ESTEBAN, M. A. 2012. Risks of using antifouling biocides 610 in aquaculture. Int J Mol Sci, 13, 1541-60.
- HOU, D., HUANG, Z., ZENG, S., LIU, J., WEI, D., DENG, X., WENG, S., HE, Z. & HE, J. 2017. Environmental 611 612 Factors Shape Water Microbial Community Structure and Function in Shrimp Cultural Enclosure 613 Ecosystems. Frontiers in microbiology, 8, 2359-2359.
- JOOST, U., JUGANSON, K., VISNAPUU, M., MORTIMER, M., KAHRU, A., NÕMMISTE, E., JOOST, U., 614 615 KISAND, V. & IVASK, A. 2015. Photocatalytic antibacterial activity of nano-TiO2 (anatase)-based 616 thin films: Effects on Escherichia coli cells and fatty acids. Journal of Photochemistry and 617 Photobiology B: Biology, 142, 178-185.
  - JORGENSEN, S. L., HANNISDAL, B., LANZÉN, A., BAUMBERGER, T., FLESLAND, K., FONSECA, R., ØVREÅS, L., STEEN, I. H., THORSETH, I. H., PEDERSEN, R. B. & SCHLEPER, C. 2012. Correlating microbial community profiles with geochemical data in highly stratified sediments from the Arctic Mid-Ocean Ridge. Proceedings of the National Academy of Sciences, 109, E2846.
    - KADIYALA, U., KOTOV, N. A. & VANEPPS, J. S. 2018. Antibacterial Metal Oxide Nanoparticles: Challenges in Interpreting the Literature. Curr Pharm Des, 24, 896-903.
    - KAHRILAS, G. A., BLOTEVOGEL, J., STEWART, P. S. & BORCH, T. 2015. Biocides in hydraulic fracturing fluids: a critical review of their usage, mobility, degradation, and toxicity. Environ Sci Technol, 49,
  - KANCHI, S. & KHAN, A. Biogenic Synthesis of Selenium Nanoparticles with Edible Mushroom Extract: Evaluation of Cytotoxicity on Prostate Cancer Cell Lines and Their Antioxidant, and Antibacterial Activity. 2020.
- 630 KIM, J. Y., PARK, J. H., KIM, M., JEONG, H., HONG, J., CHUCK, R. S. & PARK, C. Y. 2017. Safety of Nonporous Silica Nanoparticles in Human Corneal Endothelial Cells. Sci Rep., 7, 14566.
  - KRUG., H. F. 2008. Working Report on the Status Quo of Nanomaterials Impact on Human Health and the Environment - Improving the understanding of the impact of nanoparticles on human health and the environment. ImPart.
  - KUMARI, J., KUMAR, D., MATHUR, A., NASEER, A., KUMAR, R. R., THANJAVUR CHANDRASEKARAN, P., CHAUDHURI, G., PULIMI, M., RAICHUR, A. M., BABU, S., CHANDRASEKARAN, N., NAGARAJAN, R. & MUKHERJEE, A. 2014. Cytotoxicity of TiO2 nanoparticles towards freshwater sediment microorganisms at low exposure concentrations. Environ Res, 135, 333-45.
- 639 LEVY, S. B. 2002. Active efflux, a common mechanism for biocide and antibiotic resistance. Journal of 640 Applied Microbiology, 92, 65s-71s.
- 641 LI, Q., MAHENDRA, S., LYON, D. Y., BRUNET, L., LIGA, M. V., LI, D. & ALVAREZ, P. J. 2008. Antimicrobial 642 nanomaterials for water disinfection and microbial control: potential applications and 643 implications. Water Res, 42, 4591-602.
- 644 LIU, Y., TAN, J., THOMAS, A., OU-YANG, D. & MUZYKANTOV, V. R. 2012. The shape of things to come: 645 importance of design in nanotechnology for drug delivery. Ther Deliv, 3, 181-94.
- 646 LIU, Z. H., ZHOU, H. F., LIU, J. F., HUANG, M., YIN, X. D., LIU, Z. S., MAO, Y. F., XIE, W. Y. & LI, D. H. 2018. 647 Evaluation of performance and microbial community successional patterns in an integrated OCO 648 reactor under ZnO nanoparticle stress. Rsc Advances, 8, 26928-26933.
- 649 LONDONO, N., DONOVAN, A. R., SHI, H., GEISLER, M. & LIANG, Y. 2017. Impact of TiO2 and ZnO 650 nanoparticles on an aquatic microbial community: effect at environmentally relevant 651 concentrations. Nanotoxicology, 11, 1140-1156.
- 652 LOVE, M. I., HUBER, W. & ANDERS, S. 2014. Moderated estimation of fold change and dispersion for 653 RNA-seq data with DESeq2. *Genome Biol,* 15, 550.

- 654 MAILLARD, J. Y. 2005. Antimicrobial biocides in the healthcare environment: efficacy, usage, policies, 655 and perceived problems. *Ther Clin Risk Manag*, **1**, 307-20.
- 656 MCMURDIE, P. J. & HOLMES, S. 2013. phyloseq: an R package for reproducible interactive analysis and 657 graphics of microbiome census data. *PLoS One*, 8, e61217.
  - MOLL, J., KLINGENFUSS, F., WIDMER, F., GOGOS, A., BUCHELI, T. D., HARTMANN, M. & VAN DER HEIJDEN, M. G. A. 2017. Effects of titanium dioxide nanoparticles on soil microbial communities and wheat biomass. *Soil Biology & Biochemistry*, 111, 85-93.
  - MUMFORD, A. C., AKOB, D. M., KLINGES, J. G. & COZZARELLI, I. M. 2018. Common Hydraulic Fracturing Fluid Additives Alter the Structure and Function of Anaerobic Microbial Communities. *Appl Environ Microbiol*, 84, e02729-17.
  - PANACEK, A., KVITEK, L., SMEKALOVA, M., VECEROVA, R., KOLAR, M., RODEROVA, M., DYCKA, F., SEBELA, M., PRUCEK, R., TOMANEC, O. & ZBORIL, R. 2018. Bacterial resistance to silver nanoparticles and how to overcome it. *Nat Nanotechnol*, 13, 65-71.
  - PARADA, A. E., NEEDHAM, D. M. & FUHRMAN, J. A. 2016. Every base matters: assessing small subunit rRNA primers for marine microbiomes with mock communities, time series and global field samples. *Environ Microbiol*, 18, 1403-14.
  - PATERSON, G., ATARIA, J. M., HOQUE, M. E., BURNS, D. C. & METCALFE, C. D. 2011. The toxicity of titanium dioxide nanopowder to early life stages of the Japanese medaka (Oryzias latipes). *Chemosphere*, 82, 1002-9.
  - RIPOLLES-AVILA, C., MARTINEZ-GARCIA, M., HASCOËT, A.-S. & RODRÍGUEZ-JEREZ, J. J. 2019. Bactericidal efficacy of UV activated TiO2 nanoparticles against Gram-positive and Gram-negative bacteria on suspension. *CyTA Journal of Food*, 17, 408-418.
  - SCHNEIDER, J., MATSUOKA, M., TAKEUCHI, M., ZHANG, J., HORIUCHI, Y., ANPO, M. & BAHNEMANN, D. W. 2014. Understanding TiO2 photocatalysis: mechanisms and materials. *Chem Rev*, 114, 9919-86.
  - SIDDIQUI, A., PINEL, I., PREST, E. I., BUCS, S. S., VAN LOOSDRECHT, M. C. M., KRUITHOF, J. C. & VROUWENVELDER, J. S. 2017. Application of DBNPA dosage for biofouling control in spiral wound membrane systems. *Desalin Water Treat*, 68, 12-22.
  - SLAVIN, Y. N., ASNIS, J., HÄFELI, U. O. & BACH, H. 2017. Metal nanoparticles: understanding the mechanisms behind antibacterial activity. *Journal of nanobiotechnology*, 15, 65-65.
  - TECHTMAN, S. M., MAHMOUDI, N., WHITT, K. T., CAMPA, M. F., FORTNEY, J. L., JOYNER, D. C. & HAZEN, T. C. 2017. Comparison of Thaumarchaeotal populations from four deep sea basins. *FEMS Microbiol Ecol*, 93, p. fix128.
- VIKRAM, A., BOMBERGER, J. M. & BIBBY, K. J. 2015a. Efflux as a glutaraldehyde resistance mechanism in Pseudomonas fluorescens and Pseudomonas aeruginosa biofilms. *Antimicrob Agents* Chemother, 59, 3433-40.
- 690 VIKRAM, A., BOMBERGER, J. M. & BIBBY, K. J. 2015b. Efflux as a Glutaraldehyde Resistance Mechanism 691 in Pseudomonas fluorescens and Pseudomonas aeruginosa Biofilms. *Antimicrobial Agents and Chemotherapy*, 59, 3433-3440.
  - WANG, L., HU, C. & SHAO, L. 2017. The antimicrobial activity of nanoparticles: present situation and prospects for the future. *International journal of nanomedicine*, 12, 1227-1249.
- WARD, C. S., PAN, J. F., COLMAN, B. P., WANG, Z., GWIN, C. A., WILLIAMS, T. C., ARDIS, A., GUNSCH, C. K.
   & HUNT, D. E. 2019. Conserved Microbial Toxicity Responses for Acute and Chronic Silver
   Nanoparticle Treatments in Wetland Mesocosms. *Environ Sci Technol*, 53, 3268-3276.
- 598 ZHANG, Y., CHEN, Y., WESTERHOFF, P., HRISTOVSKI, K. & CRITTENDEN, J. C. 2008. Stability of commercial metal oxide nanoparticles in water. *Water Res,* 42, 2204-12.

# Figure Legends

Fig. 1. Transmission electron microscopy photomicrograph of (A) TiO<sub>2</sub>NPs stock solution, (B) ZnO NPs stock solution, (C) SiO<sub>2</sub>NPs.

704

701

Fig.2. LDH activity for microcosms treated with 16.7 mg/L concentration of biocides and NPs after 24h incubationa nd the standard error (n=3).

707

Fig.3. Changes in microbial abundance over time. The mean and standard deviation of 16S rRNA gene copies for each timepoint of nanoparticles and biocides microcosms from in Lower Grays Run, PA samples.

711

- Fig.4. Principal coordinate analysis (PCoA) of Bray Curtis Dissimilarity of the rarified ASV
- table of microcosms from Lower Grays Run, PA samples with 16.7 mg/L concentration of three
- metal oxides NPs and biocides. This is showing the dissimilarity of the microbial community on
- day 0 (open symbols) and day 14 (closed symbols). Treatments are shown as different colors

716

- Fig. 5: Bar graph of taxonomic diversity shows the relative abundance of bacterial order with
- 718 those classes represented with different colors. This figure shows the relative abundance of
- bacterial orders on day 0 and day 14 for Lower Grays Run, PA samples incubated with three
- metal oxide nanoparticles, and biocides at 16.7 mg/L concentration for all treatments.

- 722 Supporting Information Legends
- Fig. S1. Map of Stream Site made with Google Earth.
- Fig. S2. pH measurements for microcosms during the 14-day incubation.
- Fig.S3. Three different richness and evenness alpha diversity metrics for the samples from day 0
- and day 14 (A)Shannon, (B) Inverse Simpsons, and (C) Richness (observed ASVs). Error bars
- show the standard error for determination of alpha diversity from 100 rarified tables.
- 728 Table S1 Stability of TiO<sub>2</sub>, ZnO, and SiO<sub>2</sub> nanoparticles in Lower Grays Run, PA.
- Hydrodynamic Size (d. nm) distribution at 0, 1, 7, and 14 days. (n=3) (average  $\pm$  stander error or
- 730 Standard Deviation).
- Table S2: Zeta Potential (mV) of TiO<sub>2</sub>, ZnO, and SiO<sub>2</sub> nanoparticles in Lower Grays Run, PA.
- Hydrodynamic Size (d. nm) distribution at 0, 1, 7, and 14 days. (n=3) (average  $\pm$  stander error or
- 733 Standard Deviation).
- Table S3 The statistic of the pH level of the microcosms. Shapiro-Wilk normality test,
- kruskal.test, and Dunn.test were used to compare between Biocide and Nanoparticles at 0, 1, 7,
- and 14 days to evaluate the significance relative to the control of experimental results (P<0.05).
- 737 Table S4: Dunn Test Results comparing pH by time and treatment category
- Table S5. Dunn Test comparison of time and treatment type for LDH data p-values corrected
- 739 with the Benjamini-Hochberg
- 740 Table S6. Dunn Test comparison of time and Treatment for LDH data p-values corrected with
- 741 the Benjamini-Hochberg
- 742 Table.7: The microbial abundance of the 16S rRNA gene using the quantitative Polymerase
- 743 chain reaction (qPCR).
- Table S8 Statistics of the microbial abundance of the 16S rRNA gene using the quantitative
- Polymerase chain reaction (qPCR). Shapiro-Wilk normality test, kruskal.test
- Table S9 The statistic of the microbial abundance of the 16S rRNA gene using the quantitative
- Polymerase chain reaction (qPCR). Dunn Test with p values adjusted with the Benjamini-
- 748 Hochberg correction for false discovery rate.
- 749 Table.S10: The statistic of three different richness and evenness alpha diversity, (a)Shannon,
- 750 (b)inverse Simpsons, and (c)richness (observed ASVs). One-way ANOVA was used to compare
- between Biocide and Nanoparticles at day 14 days to evaluate the significance relative to control
- of experimental results (P<0.05) in Lower Grays Run, PA samples.
- 753 Table S11: DESeq2 significantly enriched ASVs